# Origin of Inequivalent Chromium–Carbonyl Bond Lengths in Chlorotetracarbonylethylidynechromium

Arthur A. Low and Michael B. Hall*

*Department of Chemistry, Texas A&M University, College Station, Texas 77840-3325*

*Received August 3, 1989*

In the reported crystal structure of $Cl(CO)_4Cr{\equiv}CCH_3$, two distinct pairs of $Cr-C_{CO}$ bond distances are reported. The difference $Cr-C_{CO}$ bond distances were attributed to two possible effects: (1) a hyperconjugative interaction of the methyl group on the chromium atom and (2) the effects of crystal packing on the molecule. In this paper, the molecule $Cl(CO)_4Cr{\equiv}CCH_3$ is studied with use of ab initio full-gradient geometry optimization techniques in order to ascertain what causes the inequivalent $Cr-C_{CO}$ bond distances. From the results of the optimizations, it can be concluded that a tilt of the methyl group such that its local 3-fold axis is no longer collinear with the Cr≡C axis is the cause of the inequivalent $Cr-C_{CO}$ bond distances. This tilt is caused by close contacts of the methyl hydrogens with chlorine atoms of neighboring molecules, an effect of crystal packing. The tilted methyl group then induces a charge flow between the chromium and carbyne carbon atoms, which, in turn, causes the Cr–CO bond distances to differ.

## Introduction

The class of compounds $X(CO)_4MCR$ (X = Cl, Br, I; M = Cr, Mo, W; R = aryl, alkyl), containing a metal–carbon triple bond, were first reported by Fischer et al. in 1973.[1] Since that initial discovery, many compounds of this type have been reported with different R groups.[2] These complexes have been well characterized spectroscopically and structurally. These compounds are similar structurally with a nearly octahedral arrangement of ligands and with the halogen atom in a trans position relative to the carbyne. The carbonyls in the equatorial plane are bent slightly toward the halogen atom. This effect has been ascribed to the steric strain caused by the Cr≡C bond[2] and to the preference for equatorial carbonyls to bend toward the weaker $\pi$ acceptor or the stronger $\pi$ donor.[3]

The low-temperature X-ray crystal structure analysis of $Cl(CO)_4Cr{\equiv}CCH_3$ reported by Krüger et al. shows two significantly different $Cr-C_{CO}$ bond distances.[4] One pair of trans-positioned carbonyls has shorter $Cr-C_{CO}$ bond distances (average of 1.928 (3) Å) than the other pair of carbonyls (average of 1.984 (3) Å). This difference of 0.056 (6) Å is structurally significant. The hydrogen atoms of the methyl group were located and refined upon in the structural analysis. One of the hydrogen atoms was located in the plane formed by the pair of carbonyls with the shorter $Cr-C_{CO}$ bond lengths.

Two possible causes of the inequivalent $Cr-C_{CO}$ bond lengths were proposed by the authors. The location of one of the methyl hydrogens in the plane of a pair of the carbonyls led to a hypothesis that the hyperconjugative effect of the methyl group on the chromium atom, as shown in eq 1, could cause the inequivalent $Cr-C_{CO}$ bond

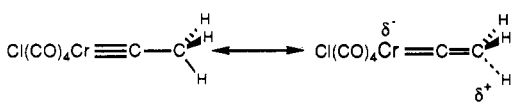


(1)

lengths. We believe that even if the rotation of the methyl group is restricted, the hyperconjugative effect of the three H atoms should be equal, thereby equilibrating the two $\pi$ bonds to the Cr atom. Unless there is something different about the coplanar hydrogen, such as a distortion of the methyl group, the hyperconjugative effect alone should not result in inequivalent Cr–C $\pi$-bonds.

Alternatively, the inequivalent $Cr-C_{CO}$ bonds could be caused by the effect of crystal packing on the molecular structure, which is the second possible cause mentioned by the authors. In the reported crystal structure, there are close nonbonding contacts between each of the methyl hydrogens and a chlorine atom from different neighboring molecules of 2.66 (2), 2.71 (2), and 2.77 (2) Å. We believe that these contacts could possibly cause a tilt of the methyl group such that the pseudo-3-fold axis of the methyl group is no longer collinear with the Cr≡C axis. This tilt could possibly cause the inequivalent $Cr-C_{CO}$ bond distances. In fact, the methyl group is actually tilted 3° in the crystal structure. However, this is probably not significantly over the error in the crystal structure. In fact, the tilt could be even larger since its measurement depends on the accurate location of the hydrogens.

A conjugative effect has been observed experimentally for the compound $X(CO)_4Cr{\equiv}CNR_2$. Both spectroscopic[5] and structural[6] observations indicate a significant contribution of the resonance form shown in eq 2. However,

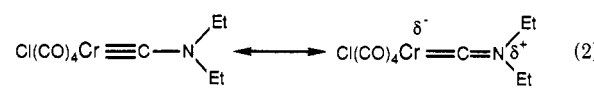


(2)

in none of the reported structures of $X(CO)_4Cr{\equiv}CNR_2$ complexes, $Br(CO)_4Cr{\equiv}CNEt_2$,[7] $Ph_3Sn(CO)_4Cr{\equiv}CNEt_2$,[8] or $Cl(CO)_4Cr{\equiv}CN(i\text{-}Pr)_2$,[9] is there a differentiation of $Cr-C_{CO}$ bond distances similar to that in $Cl(CO)Cr{\equiv}CCH_3$. This is due to the fact that, in all of the reported structures, the $NR_2$ group is not coplanar with the CO groups but rather lies approximately on a diagonal between the two sets of planar trans carbonyl groups.

A number of theoretical calculations have been performed on chromium carbyne complexes. One of the first

(1) Fischer, E. O.; Kreis, G.; Kreiter, C. G.; Müller, J.; Huttner, G.; Lorenz, H. *Angew. Chem.* **1973**, *85*, 618; *Angew. Chem., Int. Ed. Engl.* **1973**, *12*, 564.
(2) For a recent review, see: Fisher, H. *Carbyne Complexes*; VCH: New York, 1988; and references therein.
(3) Kostić, N. M.; Fenske, R. F. *Organometallics* **1982**, *1*, 489.
(4) Krüger, C.; Goddard, R.; Claus, K. H. *Z. Naturforsch.* **1983**, *38B*, 1431.
(5) Fischer, E. O.; Kreis, G.; Kreissl, F. R.; Kalbfus, W.; Winkler, E. *J. Organomet. Chem.* **1974**, *65*, C53.
(6) Fischer, E. O.; Hunter, G.; Kleine, W.; Frank, A. *Angew. Chem.* **1975**, *87*, 781; *Angew. Chem., Int. Ed. Engl.* **1975**, *14*, 760.
(7) Fischer, E. O.; Kleine, W.; Kreis, G.; Kreissl, F. R. *Chem. Ber.* **1978**, *111*, 3542.
(8) Schubert, U. *Cryst. Struct. Commun.* **1980**, *9*, 383.
(9) Fischer, H.; Motsch, A.; Märkel, R.; Ackerman, K. *Organometallics* **1985**, *4*, 726.

0276-7333/90/2309-0701$02.50/0 

was a Fenske–Hall molecular orbital study by Kostić and Fenske on *trans*-[X(CO)$_4$Cr≡CR] (X = Cl, Br, I; R = Me, Ph, NEt$_2$).[3] In their study, the carbyne ligand was described as a very strong π-acceptor, stronger even than CO. The fragment orbitals of CMe$^+$ involved in bonding to the Cr atom were described as a filled σ-type sp hybrid orbital pointing toward the Cr atom and two empty degenerate π-type orbitals. The π-type orbitals are mainly p orbitals of the carbyne carbon atom with some hyperconjugative contribution from the three C–H bonds (percent contributions of methyl $p_\pi$ and H s orbitals are 2% and 9%, respectively).[3] The CMe$^+$ fragment forms two equivalent π bonds with the metal. This is in contrast to the case for the two other fragments, CPh$^+$ and CNEt$_2^+$, which, in the case of CPh$^+$, two similar but not equal π bonds are formed due to delocalization of one of the unoccupied π-acceptor orbitals into the phenyl ring and, in the case of CNEt$_2^+$, two different π bonds are formed due to interaction of the nitrogen lone pair with one of the π-acceptor orbitals.

In a modified CNDO study on Cl(CO)$_4$Cr≡CCH$_3$,[10] the electronic properties of the CCH$_3$ ligand were compared with those of the NO radical. Also, the possibility of hyperconjugation of the methyl carbon to the carbyne carbon was indicated by a greater amount of π character in the carbyne carbon–methyl carbon bond relative to that in the methyl carbon–acetylene carbon bond of 1-propyne.

There is also experimental evidence of a hyperconjugative effect in methyl carbyne complexes of chromium. A Raman spectroscopic study of diluted isotopic species of Br(CO)$_4$Cr≡CCH$_3$ in the solid state revealed the existence of two different C–H bond strengths, which is consistent with the hyperconjugative model.[11] However, this observation could also be consistent with the crystal-packing effects being the cause of the two different C–H bond strengths.

In summary, two possible causes of the inequivalent Cr–C$_{CO}$ bond lengths have been put forward: (1) an intramolecular effect of hyperconjugation of the CH$_3$ group on the chromium atom and (2) an intermolecular effect of crystal packing on the molecule. From the results of geometry optimizations of the ab initio SCF wave function of Cl(CO)$_4$Cr≡CCH$_3$, the cause of the inequivalent Cr–C$_{CO}$ bond lengths has been ascertained.

## Theoretical Methods

The molecular orbitals were generated by using as basis functions the split valence basis set of Williamson and Hall,[12] which consists of a (14s11p5d/5s4p2d) basis for Cr, a (9s6p/4s3p) basis for Cl,[13] a (6s3p/3s2p) basis for the C and O atoms,[13] and a (3s/2s) basis for H.[13] Molecular orbitals were generated via the closed-shell Hartree–Fock Roothaan (HFR) method.[14] Geometry optimizations were performed via full-gradient methods.[15]

Two fragment analyses of Cl(CO)$_4$Cr≡CCH$_3$ were performed to obtain more information about the Cr≡C and C—CH$_3$ bonds. The first analysis used the quartet fragments obtained by homolytically breaking the Cr≡C bond. The second analysis used the doublet fragments obtained by homolytically breaking the C—CH$_3$ bond. In each analysis, the molecular wave function was analyzed in terms of the fragment orbitals.

A number of different deformation density maps were computed by subtracting various promolecules from the electron density of the complex. For what we call the "standard" deformation density, the promolecule used was the sum of the densities of the spherically averaged constituent atoms. To compute the fragment deformation density, the promolecule used in the computation consisted of spherically averaged chromium and chlorine atoms, four isolated CO molecules in the same orientation as the molecule, and a quartet CCH$_3$ fragment with one electron in each of the carbyne carbon's $p_\pi$ ($p_x$, $p_y$) and σ ($sp_z$ hybrid) orbitals.

All of the molecular orbital calculations and geometry optimizations were performed with use of GAMESS[16] package of programs. The fragment analysis was performed with use of the new program GTRAN.[17] All deformation density and molecular orbital plots were generated with use of the program MOPLOT.[18] The deformation and difference density maps are contoured linearly with an increment of 0.10 e Å$^{-3}$. Negative contours are shown by dashed lines. The absolute value of the smallest contour is 0.1 e Å$^{-3}$. The molecular orbitals are contoured geometrically with each contour differing by a factor of 2. The absolute value of the smallest contour is $\pm 2^{-7}(7.8125 \times 10^{-3})$ (e au$^{-3}$)$^{1/2}$.

All GAMESS calculations were performed at the Cornell National Supercomputer Facility by using FPS264 array processors attached to an IBM 3090-400 computer. All other calculations were performed on a VAX 11/780 computer.

## Results and Discussion

**Geometry.** The first geometry optimization was started at the crystal structure geometry, hereafter referred to as structure **1**, which had first been idealized to $C_s$ symmetry; that is, the out-of-plane Cr–C2–O2 and Cr–C4–O4 bond distances and angles and the C6–H1 and C6–H2 bond distances had been equilibrated. Then, the full geometry

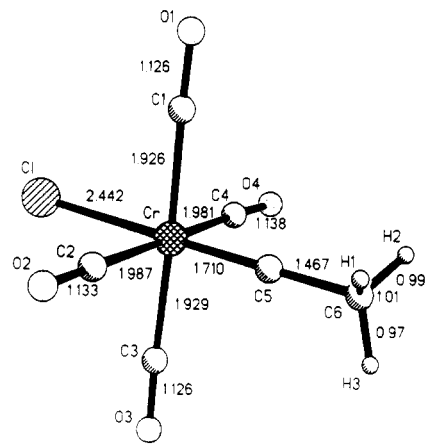


**1**

was optimized while the $C_s$ symmetry of the molecule was maintained. The resulting optimized structure will hereafter be referred to as the no-tilt structure or structure **2**.

The second geometry optimization was started at structure **2** with the methyl group tilted 12° in the direction that moves the in-plane methyl hydrogen toward the carbyne carbon. Again, the optimization was performed by retaining the $C_s$ symmetry of the molecule and now fixing the methyl's tilt at 12°. This optimized structure will hereafter be referred to as the 12°-tilt

(10) Saddei, D.; Freund, H.-J.; Hohlneicher, G. *J. Organomet. Chem.* **1981**, *216*, 235.
(11) Dao, N. Q.; Fervier, H.; Jouan, M.; Tran-Huy, N. H.; Fischer, E. O.; Neugebauer, D. *J. Organomet. Chem.* **1982**, *241*, C53.
(12) Williamson, R. L.; Hall, M. B. *Int. J. Quantum Chem., Quantum Chem. Symp.* **1987**, *21*, 503.
(13) These basis sets was based on Huzinaga's (333-33) basis for Cl, his (33-3) basis for C and O, and (3) basis for H with the most diffuse function of the s and p valence shells split. For these basis functions see: Huzinaga, S., Ed. *Gaussian Basis Sets for Molecular Calculations*; Elsevier: Amsterdam, 1984.
(14) Roothaan, C. C. J. *Rev. Mod. Phys.* **1951**, *23*, 69.
(15) Pulay, P. *Mol. Phys.* **1969**, *17*, 197.
(16) M. F. Guest, Daresbury Laboratory, U.K., provided the FPS version of GAMESS.
(17) GTRAN program written by Andrew Sargent.
(18) Lichtenberg, D. L. Ph.D. Dissertation, University of Wisconsin, Madison, WI, 1974. The program is available from the QCPE, Indiana University, Bloomington, IN 47401, Program 284.

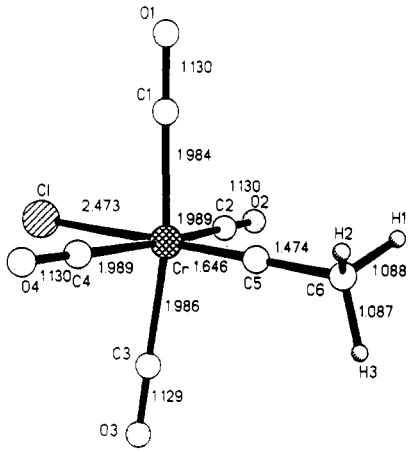


2

structure or structure 3. The bond distances from these

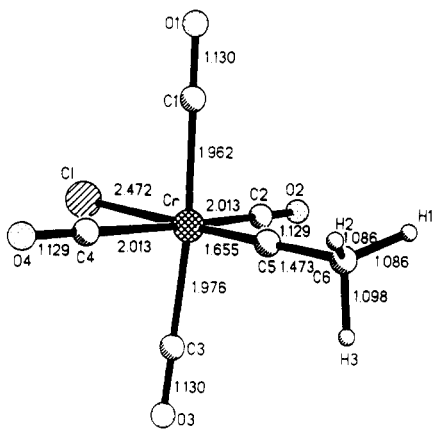


3

optimizations, as well as those from the crystal structure, are shown in the drawings. Selected bond angles are shown in Table I. The numbering of the atoms is the same as in the crystal structure analysis. The coordinate system used in the discussion that follows can be approximated as follows: the $z$ axis points along the Cr–C5(carbyne) bond; the $x$ axis points along the Cr–C1 bond; the $y$ axis points along the Cr–C4 bond.

In structure 2, all of the Cr–$C_{CO}$ bond lengths have (Cr–C1, Cr–C2, Cr–C3, Cr–C4) become essentially equivalent. The optimized Cr≡C bond distance of 1.646 Å is considerably shorter than the experimental value of 1.710 (3) Å. However, the optimized value for the Cr≡C bond length is consistent with previously theoretically optimized Cr≡C bond lengths of 1.62 Å for $Cl(CO)_4Cr{\equiv}CH$ with a minimal basis set[19] and 1.655 Å for $Cl(CO)_4Cr{\equiv}CH$ with a larger basis set.[20] Electron correlation effects need to be included to obtain a Cr≡C bond length closer to the experimental value. For example, a Cr≡C bond length of 1.710 Å is obtained from a CASSCF calculation on $Cl(CO)_4Cr{\equiv}CH$.[20] The second largest difference in the bond distances from 1 to 2 occurs for the Cr–Cl bond, which the calculation predicts to be too long by 0.03 Å. For the bond angles, the most significant difference is an increased bend of the equatorial carbonyls toward the chlorine atom, that is, decreased Cl–Cr–$C_{CO}$ angles and increased $C_{CO}$–Cr–$C_{carbyne}$ angles.

**Table I. Bond Distances and Angles in $Cl(OC)_4CrCCH_3$**

| | cryst struct | optimized struct | 12° Me tilt struct |
|---|---|---|---|
| | Bond Distances (Å) | | |
| Cr–Cl | 2.442 (1) | 2.473 | 2.472 |
| Cr–C1 | 1.926 (3) | 1.984 | 1.962 |
| Cr–C2 | 1.987 (3) | 1.989 | 2.013 |
| Cr–C3 | 1.929 (3) | 1.986 | 1.976 |
| Cr–C4 | 1.981 (3) | 1.989 | 2.013 |
| Cr–C5 | 1.710 (3) | 1.646 | 1.655 |
| C5–C6 | 1.467 (4) | 1.473 | 1.473 |
| C6–H1 | 1.01 (1) | 1.087 | 1.086 |
| C6–H2 | 0.99 (1) | 1.087 | 1.086 |
| C6–H3 | 0.97 (1) | 1.088 | 1.098 |
| | Bond Angles (deg) | | |
| Cl–Cr–C1 | 86.2 (1) | 85.2 | 86.0 |
| Cl–Cr–C2 | 89.0 (1) | 84.9 | 83.8 |
| Cl–Cr–C3 | 89.9 (1) | 84.9 | 86.3 |
| Cl–Cr–C4 | 88.8 (1) | 84.9 | 83.8 |
| Cl–Cr–C5 | 178.9 (1) | 179.9 | 180.0 |
| C1–Cr–C2 | 91.6 (1) | 89.6 | 89.7 |
| C1–Cr–C3 | 175.9 (1) | 170.1 | 172.3 |
| C1–Cr–C4 | 88.9 (1) | 89.6 | 89.7 |
| C1–Cr–C5 | 92.7 (1) | 94.9 | 92.7 |
| C2–Cr–C3 | 89.9 (1) | 89.6 | 89.4 |
| C2–Cr–C4 | 177.8 (1) | 169.8 | 167.6 |
| C2–Cr–C5 | 90.6 (1) | 95.1 | 96.2 |
| C3–Cr–C4 | 89.5 (1) | 89.6 | 89.4 |
| C3–Cr–C5 | 91.1 (1) | 95.1 | 96.2 |

In structure 3, the pattern of pairs of short and long Cr–$C_{CO}$ bond lengths reappears. Compared to the case for the no-tilt structure, the Cr–C1 and Cr–C3 bonds have shortened in structure 3 by 0.022 and 0.010 Å, respectively. These two bonds correspond to the shorter Cr–$C_{CO}$ bond lengths in the experimental structure 1. Again, compared to the case for the no-tilt structure, both the Cr–C2 and Cr–C4 bonds have lengthened in structure 3 by 0.024 Å (bond lengths are equivalent due to the $C_s$ symmetry). These two bonds correspond to the longer Cr–$C_{CO}$ bond lengths in structure 1. Other changes in bond lengths as the methyl group tilts are a lengthening of the Cr–C5 bond by 0.009 Å and a lengthening of the in-plane C6–H3 bond by 0.010 Å. Additionally, there are small changes in the Cl–Cr–$C_{CO}$ bond angles as the methyl group tilts. The carbonyls, C1O1 and C3O3, bend toward the carbyne ligand by 0.8 and 1.4°, respectively, while C2O2 and C4O4 bend toward the chlorine atom by 1.1° (again, these two carbonyls are equivalent due to the $C_s$ symmetry).

It is clear from the fully optimized structure 2 that the hyperconjugative effect alone cannot be the cause of the inequivalent Cr–$C_{CO}$ bond lengths. The symmetry of the $CCH_3$ fragment must be close to cylindrical; otherwise, the Cr–$C_{CO}$ bond lengths would be inequivalent in structure 2. A distortion, such as a tilt of the methyl group, is necessary to cause the observed experimental pattern of short and long Cr–$C_{CO}$ bond lengths.

**Electron Density.** To understand how the tilted methyl group causes the Cr–$C_{CO}$ bond lengths to change, we calculated the changes in the deformation density maps of structures 2 and 3. The standard deformation density maps of structure 2, formed by subtracting the density of the spherical atom promolecule from the density of the molecule, are shown in Figure 1. Figure 1a shows the deformation density in the $XZ$ plane for structure 2, while Figure 1b shows the deformation density in the $YZ$ plane for structure 2. These maps are contoured as for the experimental maps,[4] that is, linear contours with a contour interval of 0.01 e Å$^{-3}$, with the zero contour dot-dashed.

The experimental and theoretical maps qualitatively possess similar general features (see ref 4 for the experi-

(19) Ushio, J.; Nakatsuji, H.; Yonezawa, T. *J. Am. Chem. Soc.* **1983**, *105*, 434.

(20) Poblet, J. M.; Strich, A.; Wiest, R.; Bénard, M. *Chem. Phys. Lett.* **1986**, *126*, 169.

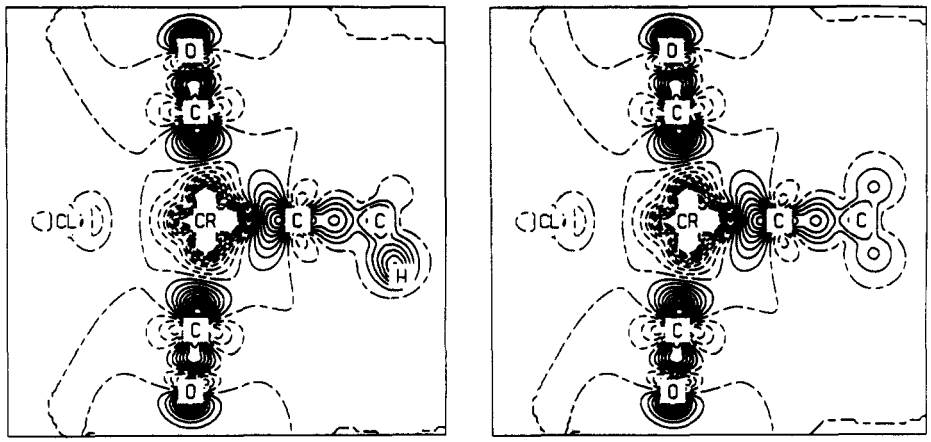


**Figure 1.** Calculated standard deformation density maps of $Cl(CO)_4Cr{\equiv}CCH_3$ in its theoretically optimized structure **2** in (a) the *XZ* plane and (b) the *YZ* plane. Maps are contoured linearly with an increment of 0.01 e Å$^{-3}$. Negative contours are shown as dashed lines. The zero contour is shown as a dot-dashed line.

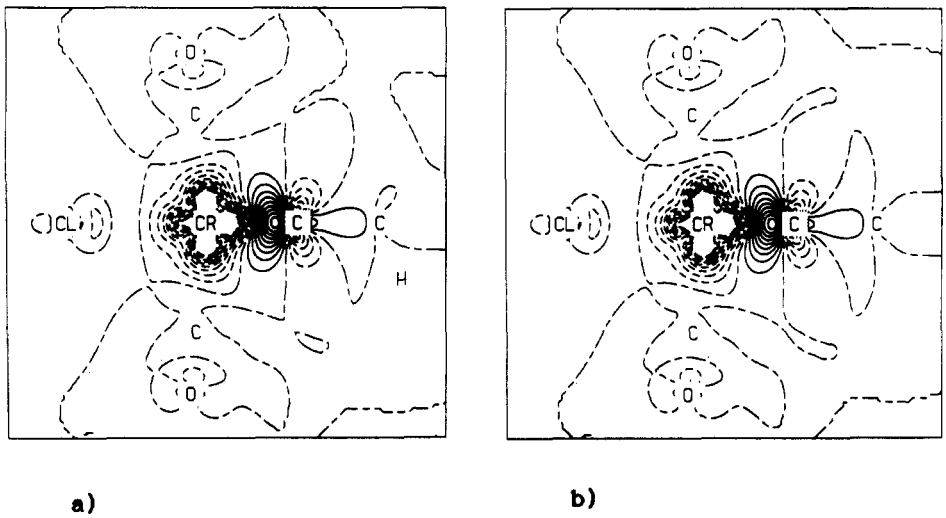


**Figure 2.** Calculated fragment deformation density maps of $Cl(CO)_4Cr{\equiv}CCH_3$ in its theoretically optimized structure **2** in (a) the *XZ* plane and (b) the *YZ* plane. Maps are contoured as in Figure 1.

mental maps). There are, however, some notable differences. The largest accumulation region in the theoretical maps occurs in the carbonyls' $5\sigma$ lone-pair regions. The second largest accumulation region occurs in the lone-pair region of the carbyne ligand. This is in contrast to the experimental maps, where the largest accumulation in the map occurs between the carbyne and methyl carbons. The accumulation between the carbyne and methyl carbons in the theoretical maps is smaller with a maximum contour level of 0.4 e Å$^{-3}$ (as opposed to 0.7 e Å$^{-3}$ in the experimental maps).

In the experimental maps, the accumulation region between the chromium and carybne carbon atoms extended toward the carbonyls' lone-pair accumulations. This extension is not seen in the theoretical maps. In the theoretical maps, the Cr≡C accumulation region is expanded out from the Cr–C axis more than the Cr–$C_{CO}$ internuclear accumulations, an indication of stronger $\pi$-bonding between the chromium and carbyne carbon.

Other notable differences between the experimental and theoretical maps are the carbonyl oxygen lone-pair accumulations, the C–H bond accumulation, and the lack of many significant features about the chlorine atom in the theoretical maps. The first two differences can be attributed to the effects of libration and thermal smearing. Obscuring of the oxygen lone-pair accumulation region in the experimental deformation densities of metal carbonyl compounds is a relatively common occurrence. However, the lack of features about the Cl atom in the theoretical maps is not so easily explained. In the experimental maps, there are accumulation regions along the Cr–Cl bond that are located closer to the Cl atom. However, in the theoretical maps, the same region corresponds to a small region of deficit. There is a very diffuse and large (in area) region of accumulation surrounding the deficit region and the Cl atom, but the amount of accumulation never amounts to more than 0.01 e Å$^{-3}$.

Often, one can see additional details if, instead of subtracting spherical atom densities, densities of molecular fragments in the same geometry as in the molecule are subtracted from the molecular density.[21] This method was used to produce fragment deformation density maps of the two structures **2** and **3**. Here, the promolecule consisted of spherically averaged chromium and chlorine atoms, the four isolated CO molecules, and a quartet fragment ($\sigma^1\pi^2$) $CCH_3$. The resultant fragment deformation density maps are shown for structure **2** in Figure 2.

(21) Sherwood, D. E.; Hall, M. B. *Inorg. Chem.* **1983**, *22*, 93.

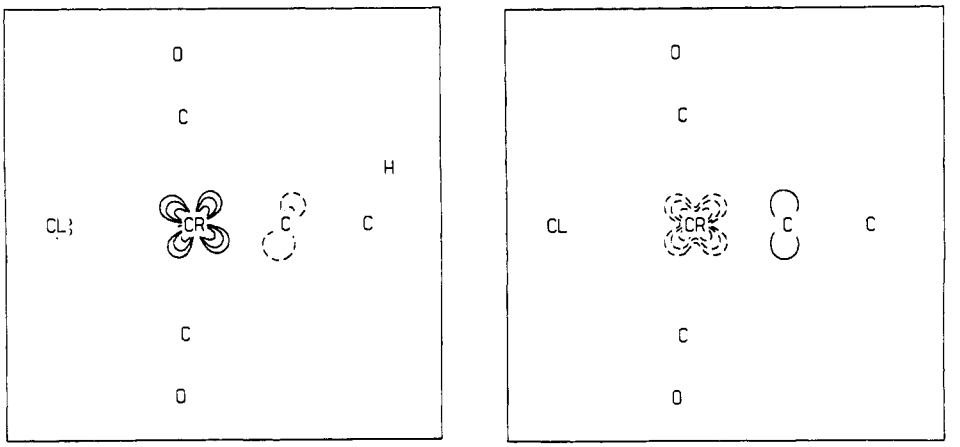


**Figure 3.** Calculated fragment difference density maps of $Cl(CO)_4Cr{\equiv}CCH_3$ obtained by subtracting the fragment deformation density maps of structure **2** from those of structure **3** in (a) the *XZ* plane and (b) the *YZ* plane. Maps are contoured as in Figure 1 with the exception that the zero contour is not shown.

Unlike the standard deformation density maps, the largest accumulation region in all the maps is now associated with the carbyne "5$\sigma$" lone pair. This accumulation region is now larger than that in the standard deformation density maps. The internuclear accumulation region between the carbyne and methyl carbons is smaller than that in the standard deformation density maps, and the deficit region corresponding to the carbyne's $p_\pi$ orbital has grown larger. These changes reflect the strong charge transfer involved in the Cr≡C bond, which could be represented as $d^6$ Cr accepting a $\sigma$ lone pair from $CCH_3^+$ ($\sigma^2\pi^0$) and donating density back to the carbyne's $\pi$ orbitals. Since, in Figure 2, the carbyne moiety is represented as $CCH_3$ ($\sigma^1\pi^2$), one sees gain in the $\sigma$ region and loss in the $\pi$ region.

The area about the chromium and chlorine atoms in the fragment deformation density maps is essentially the same as that in the standard deformation density maps. However, about the carbonyl ligands, practically all the large accumulation and deficit regions that had appeared in the standard deformation density have disappeared in the fragment deformation density maps. The only features about the carbonyl ligands are a small deficit in the CO's $\sigma$ region close to the O atom and a small accumulation in the CO's $\pi$ region of the O atom. These changes are similar to those found in the fragment deformation density maps of a carbonyl approaching a $Cr(CO)_5$ fragment by Sherwood and Hall.[21] These changes are due to the rearrangement of C–O $\sigma$ density to the 5$\sigma$ lone pair due to $\sigma$ donation to the chromium and increased $\pi$ density from $\pi$ back-bonding from the chromium atom. The large contour interval of 0.1 e Å$^{-3}$ used in these maps does not allow us to observe any of the density changes near the carbonyl carbons.

Even finer details can be observed if the fragment deformation density maps of the no-tilt structure **2** are subtracted from those of the 12°-tilt structure **3**. This procedure is preferable to subtraction of the full molecule's densities because it eliminates features which are caused by the fact that the geometries of the two molecules **2** and **3** differ. The resultant fragment difference density maps are shown in Figure 3.

These fragment difference density maps show an increase of density in the Cr $d_{xz}$ orbital and an increase of density in the carbyne carbon's $p_x$ orbital in the *XZ* plane (Figure 3a). The deficit region corresponding to the carbyne carbon's $p_x$ orbital is slightly tilted toward the coplanar C–H bond. In the *YZ* plane, an opposite charge flow is observed. There is a decrease in density in the Cr $d_{yz}$ orbital with an increase in density in the carbyne carbon's $p_y$ orbital.

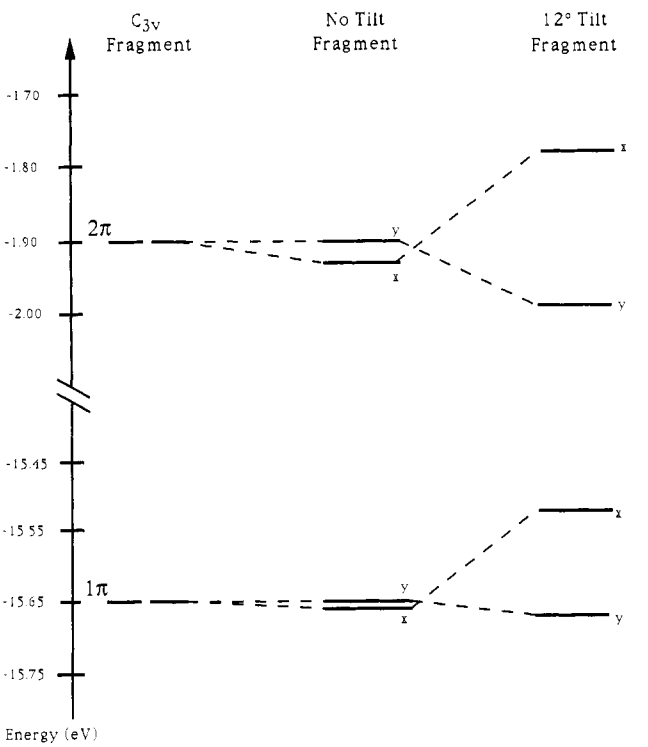


**Figure 4.** Orbital energies of the $p_{cx}$, $p_{cy}$, $\sigma_{CH_x}$, and $\sigma_{CH_y}$ orbitals of the quartet ($\sigma^1\pi^2$) $CCH_3$ fragment in various geometries.

The conclusions that can be drawn from the deformation density study is that as the methyl group is tilted, a charge flow between the chromium and carbyne carbon atoms occurs. In the *XZ* plane, charge flows from the carbyne carbon's $p_x$ orbital into the chromium's $d_{xz}$ orbital. In the *YZ* plane, density flows from the chromium $d_{yz}$ orbital into the carbyne carbon's $p_y$ orbital. The changes in density explain the change in $Cr–C_{CO}$ bond lengths as the methyl group tilts. The increased density in the Cr $d_{xz}$ orbital results in an increased amount of $\pi$ back-bonding to the in-plane carbonyl, which shortens the $Cr–C_{CO}$ bond lengths. Conversely, the decrease in density in the Cr $d_{yz}$ orbital decreases the amount of $\pi$ back-bonding to the

in-plane carbonyls, which lengthens the Cr–$C_{CO}$ bond lengths.

**Orbital Analysis.** There are two ways in which the tilt of the methyl group could cause the observed charge flow between the chromium and carbyne carbon atoms in the difference density maps. Both explanations can be obtained by observing what occurs to the fragment orbitals of the $CCH_3$ fragment as the methyl group tilts. As stated earlier, the $CCH_3$ fragment's bonding capabilities have been compared to those of a NO ligand.[10] It possesses a set of $\pi$-acceptor orbitals that consist mainly of the carbyne carbon's $p_\pi$ orbital with a small antibonding contribution from the e set of the methyl's C–H bonds. These $\pi$-acceptor orbitals shall be referred to as $p_{cx}$ and $p_{cy}$ orbitals. Lower down in energy, there is a degenerate pair of orbitals that consist mainly of the e-symmetry combination of the methyl's C–H bonds with a small bonding contribution from the respective carbyne carbon's coplanar $p_\pi$ orbital. This latter set of orbitals are reminiscent of the NO ligand's $\pi$-bonding orbitals. They shall be referred to as $\sigma_{CH_x}$ and $\sigma_{CH_y}$ orbitals.

One could analyze the system using either a valence bond or molecular orbital approach. In the valence bond approach, as the methyl group tilts, the overlap between the "in-plane" C–H bond (or the C–H bond in the *XZ* plane) and the carbyne carbon's $p_x$ orbital increases. Thus, the $\sigma_{CH_x}$ orbital has stronger $\pi$ bonding between the carbyne carbon and methyl group. This increased interaction of the carbyne carbon's $p_x$ orbital with the C–H bond decreases the amount of $\pi$ back-bonding from the metal to the carbyne carbon in the *XZ* plane. The reduced $\pi$ back-bonding results in the charge flow described above. This interaction can be described as the hyperconjugative effect shown in eq 1.

In the MO approach one looks at the $p_{cx}$ $\pi$-acceptor orbital. As the methyl tilts, there is an increased antibonding interaction between the in-plane C–H bond and the carbyne carbon's $p_x$ orbital in the $p_{cx}$ orbital. This raises the energy of the $p_{cx}$ orbital, which also results in decreased $\pi$ back-bonding from the metal to the carbyne ligand. Once again, the reduced amount of $\pi$ back-bonding in the *XZ* plane results in the observed charge flow between the chromium and carbyne carbon atoms.

The differences in overlap populations between the orbital of the carbyne carbon atom and the orbitals of both the chromium and methyl carbon atoms as the methyl group tilts should give some information about the interactions that occur. A decrease in overlap population indicates a decrease in the amount of bonding interaction between the two orbitals, whereas an increase in overlap population indicates an increase in the bonding interaction.

The largest change in the overlap populations between the orbitals of the chromium and carbyne carbon atoms occurs between the Cr $p_x$ and C5 $p_x$ orbitals. The Cr($p_x$)–C5($p_x$) overlap population decreases by 0.041 as the methyl tilts. The next two largest changes occur for the Cr($p_y$)–C5($p_y$) overlap population, which increases by 0.034, and the Cr($d_{xz}$)–C5($p_x$) overlap population, which decreases by 0.031. These changes in overlap populations between the orbitals of the chromium and the carbyne carbon would seem to suggest that the $\pi_x$-bonding interaction decreases and the $\pi_y$-bonding interaction increases between the chromium and the carbyne carbon as the methyl group tilts.

Between the orbitals of the carbyne and methyl carbon atoms, the largest change in the overlap population as the methyl group tilts occurs for the C5($p_x$)–C6($p_x$) overlap, which increases by 0.024. The next largest change occurs for the C5($p_y$)–C6($p_y$) overlap, which decreases by 0.014. The changes in overlap population indicate that as the methyl tilts, the $\pi_x$-bonding interaction between the methyl and carbyne carbon atoms increases while the $\pi_y$-bonding interaction decreases.

As with deformation density maps, we can learn more about the molecular wave function if we analyze the wave function in terms of fragment orbitals. Two different fragment analyses were performed on structures **2** and **3** in order to examine both the Cr≡C bond and the C5—C6 bond. The first analysis broke the molecule at the Cr≡C bond to produce the two quartet ($\sigma^1\pi^2$) fragments ($Cl(CO)_4Cr$ and $CCH_3$). Both structures **2** and **3** were analyzed by using fragments that have the same geometries as the respective parent molecule. Our description of the interaction of the two fragments to form the Cr≡C bond would be very similar to that given in the earlier CNDO analysis.[10] In fact, the top seven filled molecular orbitals of the SCF wave function correspond with the top seven filled molecular orbitals of the CNDO calculation. These seven MO's include the $\pi$-bonding interactions of the Cl, Cr, and carbyne carbon atoms, the Cl–Cr and Cr–$C_{carbyne}$ $\sigma$ interactions, and the Cr atom's $d_{xy}$ orbital interaction with the equatorial carbonyls. Since the origin of all the changes can be found in the $CCH_3$ fragment, it would be useful to compare the different $CCH_3$ fragments as the methyl group tilts.

The orbitals of the quartet $CCH_3$ fragment have been discussed earlier in the Results and Discussion. The $\pi$-accepting $p_{cx}$ and $p_{cy}$ orbitals are singly occupied in the fragment, whereas the $\sigma_{CH_x}$ and $\sigma_{CH_y}$ orbitals are doubly occupied. The singly occupied $\sigma$-type orbital consists mainly of a carbyne carbon $sp_z$ hybrid orbital that points toward the vacant coordination site of the carbyne carbon, much like the $5\sigma$ orbital of a NO ligand.

As the methyl group tilts, changes occur in the energy of certain orbitals of the $CCH_3$ fragment. In the *XZ* plane, the energies of the $p_{cx}$ and $\sigma_{CH_x}$ orbitals increase by 0.17 and 0.15 eV, respectively. In the *YZ* plane, the energies of the $p_{cy}$ and $\sigma_{CH_y}$ orbitals decrease by 0.10 and 0.02 eV, respectively. Additionally the energy of the $5\sigma$ orbital decreases 0.06 eV as the methyl group tilts.

The simple analysis given at the beginning of this section would lead one to expect the energy of the $\sigma_{CH_x}$ orbital to decrease and that of the $p_{cx}$ orbital to increase with the tilt of the methyl group. The cause of the rise in energy of both the $p_{cx}$ and $\sigma_{CH_x}$ orbitals can be observed in the orbital plots of the orbitals of both structures, shown in Figure 5. The plot of the $\sigma_{CH_x}$ orbital from the no-tilt structure shows that it consists mainly of the methyl carbon's $p_x$ and the in-plane hydrogen's s orbital with a small bonding contribution from the carbyne carbon's $p_x$ orbital. The plot of the $p_{cx}$ orbital from the no-tilt structure shows that it consists mainly of the carbyne carbon's $p_x$ orbital plus a small antibonding contribution from the methyl carbon's $p_x$ and the in-plane hydrogen's orbitals. Additionally, some $\sigma$ character is mixed into the $p_{cx}$ orbital. The added $\sigma$ character results in the negative lobes near the carbyne and methyl carbons almost merging together between the two carbon atoms.

As the methyl group tilts, the two orbitals in the *XZ* plane change drastically. The plot of the $\sigma_{CH_x}$ orbital shows that the interaction between the carbyne carbon and the methyl carbon p orbitals is reduced drastically on the side of the in-plane hydrogen atom but increases on the opposite side. The changes can be attributed to greater mixing in of $\sigma$ character into this orbital and increased constructive overlap between the C–H bond and the car-

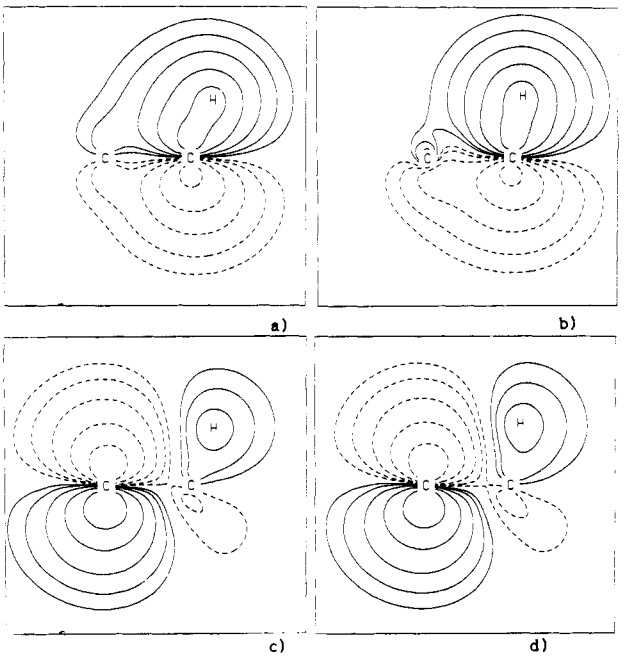


**Figure 5.** Orbital plots of the $p_{cx}$ and $\sigma_{CH_x}$ orbitals of the quartet ($\sigma^1\pi^2$) fragment of $CCH_3$: (a) the $p_{cx}$ orbital from the no-tilt structure; (b) the $p_{cx}$ orbital from the 12°-tilt structure; (c) the $\sigma_{CH_x}$ orbital from the no-tilt structure; (d) the $\sigma_{CH_x}$ orbital from the 12°-tilt structure. Orbital plots are contoured geometrically with each contour differing by a factor of 2. The absolute value of the smallest contour is $\pm 2^{-7}(7.8125 \times 10^{-3})$ (e au$^{-3}$)$^{1/2}$.

byne carbon's $p_x$ orbital as the methyl group tilts. The $p_{cx}$ orbital shows an increased destructive overlap between the C–H bond and the carbyne carbon's $p_x$ orbital as well as an increased $\sigma$ character as the methyl group tilts. From these plots, it can be concluded that as the methyl tilts, the $p_{cx}$ orbital rises in energy due to an increased antibonding interaction between the in-plane hydrogen s orbital and the carbyne carbon's $p_x$ orbital. The energy of the $\sigma_{CH_x}$ orbital probably rises due to $\sigma$ mixing into the orbital as the methyl tilts. Thus, from the orbital plots of the two $CCH_3$ fragments, the increased destructive interference of the $p_{cx}$ orbital in the tilted structure can plainly be observed. However, increased $\sigma$ mixing into the $\sigma_{CH_x}$ orbital of the tilted $CCH_3$ fragment masks the expected increased $\pi$-bonding interaction between the two carbon atoms in this orbital.

Coming back to the fragment analysis of the two quartet $Cl(CO)_4Cr$ and $CCH_3$ fragments, the fragment orbitals of the $Cl(CO)_4Cr$ fragment that form the Cr≡C bond are denoted as Cr *XZ*, Cr *YZ*, and Cr $Z^2$. They are named after the largest atomic orbital contribution to the respective fragment orbital. The Cr *XZ* and Cr *YZ* fragment orbitals form the two $\pi$ bonds with the carbyne, while the Cr $Z^2$ orbital forms the $\sigma$ bond. From the $CCH_3$ fragment, the fragment orbitals that form the Cr≡C bond are denoted as $\sigma_c$, $p_{cx}$, and $p_{cy}$. As a reminder, the *XZ* plane contains the in-plane hydrogen atom. The $\sigma_c$ fragment orbital forms the Cr–C $\sigma$ bond, while the $p_{cx}$ and $p_{cy}$ orbitals form the $\pi$ bonds with the Cr atom. As the methyl group tilts, there are substantial changes in the Mulliken populations of the fragment orbitals in the molecular wave function. In the *XZ* plane, the Mulliken population of the Cr *XZ* orbital increases 0.194 electron (e) while that of the $p_{cx}$ orbital decreases 0.176 e. Because of the tilt, the $p_{cx}$ orbital is higher in energy and therefore a poorer acceptor. In the *YZ* plane, the Mulliken population of the Cr *YZ* orbital decreases 0.193 e while that of the $p_{cy}$ orbital increases 0.172 e. Not surprisingly, these changes in Mulliken population follow the charge flow that was observed in the deformation density studies.

In summation, from the different analyses of the wave functions of $Cl(CO)_4Cr{\equiv}CCH_3$ in the two structures **2** and **3**, some conclusions may be made about the cause of the inequivalent Cr–$C_{CO}$ bond distances in the experimental geometry of $Cl(CO)_4Cr{\equiv}CCH_3$. It is most definitely caused by a tilt of the methyl group. This tilt induces a flow of charge density from the carbyne's $p_\pi$ orbital into the chromium's $d_\pi$ orbital in the plane containing the "in-plane" hydrogen. This "extra" charge density in the chromium's $d_\pi$ orbital will result in greater $\pi$ back-bonding to the in-plane carbonyls, which will shorten the Cr–$C_{CO}$ bond distances. In the perpendicular plane, an opposite charge flow occurs from the chromium's $d_\pi$ orbital to the carbyne carbon's $p_\pi$ orbital. The "loss" of charge density in the chromium's $d_\pi$ orbital in this plane results in less $\pi$ back-bonding to the in-plane carbonyl ligands, which lengthens the Cr–$C_{CO}$ bond distances in this plane. The flow of charge density between the chromium and carbyne carbon atoms as the methyl group tilts can be observed in the theoretical deformation density maps and in the fragment analysis, which splits the Cr≡C bond.

As noted earlier, inclusion of correlation is essential in order to obtain a Cr≡C bond length close to the experimentally determined bond length. One might hypothesize on how the inclusion of correlation would effect the observed charge density changes shown in this study. First, let us point out that a complete description of the Cr≡C bond is not essential for our arguments. These arguments are dependent only on the charge flow between the chromium and carbyne carbon atoms being described correctly by the SCF wave function.

In the CASSCF study of $Cl(CO)_4Cr{\equiv}CH$,[20] the Cr≡C $\pi$, $\pi^*$, $\sigma$, and $\sigma^*$ orbitals were included in the active space to obtain an equilibrium Cr≡C bond length of 1.718 Å. When the highest occupied and lowest unoccupied orbitals of $b_2$ symmetry were added to the active space, representing the Cr $d_{xy}$ ($\delta$) orbital, the equilibrium bond length decreased to 1.710 Å. Both studies resulted in significantly longer Cr≡C bond lengths from the optimized Cr–C bond lengths from SCF wave functions. However, the net charge flow between the carbyne carbon and chromium atoms does not change much, as indicated by the similar net negative charge on the carbyne carbon of –0.39 e in the CASSCF calculation (versus –0.34 e in the SCF calculation). The total amount of charge transfer between the two atoms increases, however, as indicated by the larger $p_\pi$ population on the carbyne carbon in the CASSCF wave function (1.71 vs 1.52 e in the SCF wave function) and the decreased $\sigma$ population on the carbyne carbon (4.68 e (CASSCF) vs 4.82 e (SCF)). From these observations, one can speculate that inclusion of correlation would, if anything, increase the observed effects of a tilting of the methyl group on the chromium atom.

**Similar Effects in Other Carbyne Complexes.** Because the hyperconjugative effect of the methyl group on the chromium atom is symmetric with respect to the carbonyl ligands in structure **2** of $Cl(CO)_4Cr{\equiv}CCH_3$, the Cr–$C_{CO}$ bond lengths are equivalent. It takes a tilt of the methyl group to make the effect asymmetric and to induce a differentiation of the Cr–$C_{CO}$ bond lengths. In the case of another carbyne complex, $Cl(CO)_4Cr{\equiv}CNR_2$, the conjugative effect of the $NR_2$ group on the chromium atom would be asymmetric with respect to the carbonyl groups when the trigonal $NR_2$ plane is coplanar with a pair of trans carbonyls. As noted in the Introduction, all of the reported structures of aminocarbyne complexes possess

equivalent $Cr-C_{CO}$ bond distances because the trigonal $NR_2$ group lies between the two planes of the carbonyls, thereby making the conjugative effect of the $NR_2$ group equivalent with respect to the carbonyls.

In order to investigate whether the conjugative effect in $Cl(CO)_4Cr{\equiv}CNR_2$ could induce inequivalent $Cr-C_{CO}$ bond lengths, a geometry optimization was performed on the compound $Cl(CO)_4Cr{\equiv}CNH_2$. The optimization was started with $Cr-C_{CO}$ bond lengths equal to the average $Cr-C_{CO}$ bond length in structure **2** (1.987 Å), the Cr—Cl and Cr≡C bond lengths from **2** (2.473 and 1.646 Å, respectively), and the experimental C—N bond length of 1.29 Å.[7] The geometry was optimized by holding the trigonal $NH_2$ group in the plane of a pair of trans carbonyls and maintaining the $C_{2v}$ symmetry of the molecule. Independent bond lengths from the optimized structure are shown in **4**.

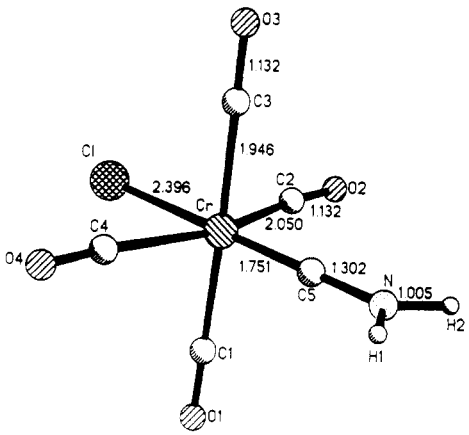


**4**

A comparison of structure **4** with structure **3** shows that the differentiation in $Cr-C_{CO}$ bond lengths is substantially larger in the aminocarbyne complex (a difference of 0.104 Å between long and short $Cr-C_{CO}$ bond distances for **4** compared to differences of 0.051 and 0.037 Å for **3**). This is an indication of the stronger conjugative effect of the $NH_2$ group on the chromium atom when compared to that of the tilted methyl group in structure **3**. Additionally, the Cr–C5 bond in structure **4** lengthens considerably from the optimized Cr–C5 bond lengths of 1.655 Å in structure **3** and 1.646 Å in structure **2**. Once again, this is an indication of the stronger conjugative effect of the $NH_2$ group on the Cr–C5 bond.

From the optimized structure **4**, one would expect to observe a lengthening of the $Cr-C_{carbyne}$ bond in the aminocarbyne complexes. The influence of the conjugative effect on the $Cr-C_{carbyne}$ bond by the $NH_2$ group would be similar no matter how the trigonal plane of the $NH_2$ group is positioned with respect to the carbonyl ligands. However, the experimental Cr≡C bond lengths in the reported aminocarbyne complexes are essentially the same as those reported for the ethylidyne complexes. It would seem that the influence of the conjugative effect on the $Cr-C_{carbyne}$ bond is overestimated at this level of calculation, that is, no correlation effects and no polarization functions. If correlation effects and polarization functions were included, the Cr–C5 bond length would probably not be as sensitive to the hyperconjugative effect. However, the same trends would be expected from the conjugative effect on the $Cr-C_{CO}$ bond lengths even if correlation effects and polarization functions are included.

## Conclusions

From the results of ab initio full-gradient geometry optimizations of $Cl(CO)_4Cr{\equiv}CCH_3$, it can be concluded that the cause of the inequivalent $Cr-C_{CO}$ bond distances in the low-temperature X-ray structural analysis of this compound is a tilt of the methyl group. This tilt is, in turn, caused by nearest-neighbor close nonbonding contacts, an intermolecular effect.

The tilt of the methyl group causes the inequivalent $Cr-C_{CO}$ bond distances by inducing (1) a charge flow from the carbyne's $\pi_x^*$ orbital (containing the in-plane C–H bond) toward the chromium's $d_{xz}$ orbital, which results in shorter $Cr-C_{CO}$ bond distances in the *XZ* plane, and (2) an opposite charge flow in the perpendicular plane, from the chromium's $d_{yz}$ orbital toward the carbyne's $\pi_y^*$ orbital, which results in longer $Cr-C_{CO}$ bond distances in the *YZ* plane. This charge flow occurs for two reasons: first, a $\pi-\pi$ bonding interaction between the carbyne and methyl carbon $p_x$ orbitals, and second, a $\pi-\pi$ antibonding interaction between the in-plane C–H bond and the carbyne carbon's $p_x$ orbital. The calculations indicate that both processes are occurring as the methyl group tilts.

**Acknowledgment.** We thank the National Science Foundation (Grant No. CHE 86-19420) and the Robert A. Welch Foundation (Grant No. A-648) for financial support. In addition, we thank C. Krüger and R. Goddard for furnishing us with the crystal structure data for $Cl(CO)_4Cr{\equiv}CCH_3$ and M. F. Guest for providing the GAMESS package of programs. This research was conducted in part with use of the Cornell National Supercomputer Facility, a resource for the Center for Theory and Simulation in Science and Engineering at Cornell University, which is funded in part by the National Science Foundation, New York State, and the IBM Corp.